Using cellular automata to simulate wildfire propagation and to assist in fire management

Joana Gouveia Freire[1] **and Carlos Castro DaCamara**[1]

[1]Instituto Dom Luiz (IDL), Faculdade de Ciências, Universidade de Lisboa, 1749-016 Lisboa, Portugal

Correspondence: Joana Freire (jcfreire@fc.ul.pt)

Abstract. Cellular Automata have been successfully applied to simulate the propagation of wildfires with the aim of assisting fire managers in defining fire suppression tactics and in planning fire risk management policies. We present a Cellular Automata designed to simulate a severe wildfire episode that took place in Algarve (southern Portugal) in July 2012. During the episode almost 25 thousand hectares burned and there was an explosive stage between 25 and 33 h after the onset. Results obtained show that the explosive stage is adequately modeled when introducing a wind propagation rule where fire is allowed to spread to non-adjacent cells depending on wind speed. When this rule is introduced, deviations in modeled time of burning (from estimated time based on hotspots detected from satellite) have a root mean square difference of 7.1 for a simulation period of 46 h (i.e. less than 20%). The simulated pattern of probabilities of burning as estimated from an ensemble of 100 simulations shows a marked decrease out of the limits of the observed scar, indicating that the model represents an added value in what respects to the choice of locations to allocate resources for fire fighting.

1 Introduction

Wildfires in the Mediterranean region have severe damaging effects that are mainly caused by large fire events (Amraoui et al., 2013, 2015). Restricting to Portugal, wildfires have burned over 1.4 million hectares in the last decade (Sá and Pereira, 2011), and the recent tragic events caused by the megafires of June and October 2017 have left a deep mark at the political, social, economic and environmental levels. Given the increasing trend in both extent and severity of wildfires (Pereira et al., 2005; Trigo et al., 2005; Pereira et al., 2013; DaCamara et al., 2014; Panisset et al., 2017), the availability of modeling tools of fire episodes is of crucial importance.

Wildfire propagation is described in a variety of ways, be it the type of modelling (deterministic, stochastic), type of mathematical formulation (continuum, grid-based) or type of propagation (nearest-neighbor, Huygens wavelets), and often the formulation adopted combines different approaches (Sullivan, 2009; Alexandridis et al., 2011). For instance, the classic model of Rothermel (1972, 1983) combines fire spread modeling with empirical observations, and simplified descriptions such as FARSITE (Finney, 2004) neglect the interaction with the atmosphere, and the fire front is propagated using wavelet techniques. Cellular Automata (CA) are one of the most important stochastic models (Sullivan, 2009); space is discretized into cells, and physical quantities take on a finite set of values at each cell. Cells evolve in discrete time according to a set of transition rules, and the states of the neighboring cells.

CA models for wildfire simulation prescribe local, microscopic interactions typically defined on a square (Clarke et al., 1994) or hexagonal (Trunfio, 2004) grid. The complex macroscopic fire spread dynamics is simulated as a stochastic process, where the propagation of the fire front to neighboring cells is modelled via a probabilistic approach. CA models directly incorporate spatial heterogeneity in topography, fuel characteristics and meteorological conditions, and they can easily accommodate any empirical or theoretical fire propagation mechanism, even complex ones (Collin et al., 2011). CA models can also be coupled with existing forest fire models to ensure better time accuracy of forest fire spread (Rui et al., 2018). More elaborated CA models that overcome typical constraints imposed by the lattice (Trunfio et al., 2011; Ghisu et al., 2015) perform comparably to deterministic models such as FARSITE, however at a higher computational cost.

In the present work, we set up a simple and fast CA model designed to simulate wildfires in Portugal. As benchmark, we have chosen the CA model developed by Alexandridis et al. (2008, 2011) that presents the advantage of having been successfully applied to other Mediterranean ecosystems, namely to the propagation of historical fires in Greece to simulate fire suppression tactics and to design and implement fire risk management policies. This model further offers the possibility to run a very high number of simulations in a short amount of time, and is easily modified by implementing additional variables and different rules for the evolution of the fire spread.

We then present and discuss the application of the CA model to the "Tavira wildfire" episode in which approximately 24,800 ha were burned in Algarve, a province located at the southern coast of Portugal. The event took place in summer 2012, between July 18 and 21, and fire spread in the municipalities of Tavira and São Brás de Alportel. The Tavira wildfire was one of the largest fires in recent years (excluding the megaevents of the last fire season of 2017), and most of the variables (e.g. total burned area, time to extinction) are well documented and available from official authorities (ANPC, 2012; Viegas et al., 2012). This fire event was also studied by Pinto et al. (2016), providing a suitable setup for testing the CA model. In addition, comparing the simulation results to this baseline scenario allowed us to identify and formulate the most promising model modifications and refinements to be incorporated in the simulation algorithm.

This paper is organized as follows. Section 2 provides a description of the fire event to be modeled and of all data required for simulation and validation of results, and also gives an overview of the rationale behind the setting up of the Cellular Automata. Results obtained are presented in Section 3, and a discussion is made in Section 4, paying special attention to the modeled temporal and spatial deviations from results derived from location and time of detection of hotspots as identified from remote sensing. Summary and conclusions are drawn in Section 5.

2   Data and methods

2.1   The fire event of Tavira

As mentioned in the introduction, we apply a CA model to a large and well documented wildfire that occurred in July 2012 in the Tavira and São Brás de Alportel municipalities, located in Algarve, Portugal (Figure 1). The fire was first reported on July 18 (at about 13 : 00 UTC) and was considered as contained on July 21 (at about 17 : 00 UTC). The fire burned approximately 24,800 ha, mainly shrublands which made up about 64% of the affected area, and spread in heterogeneous, undulated terrain. It was the largest wildfire in Portugal in 2012, contributing to more than 22% of the total amount of 110,232 ha of burned area (ICNF, 2012) in
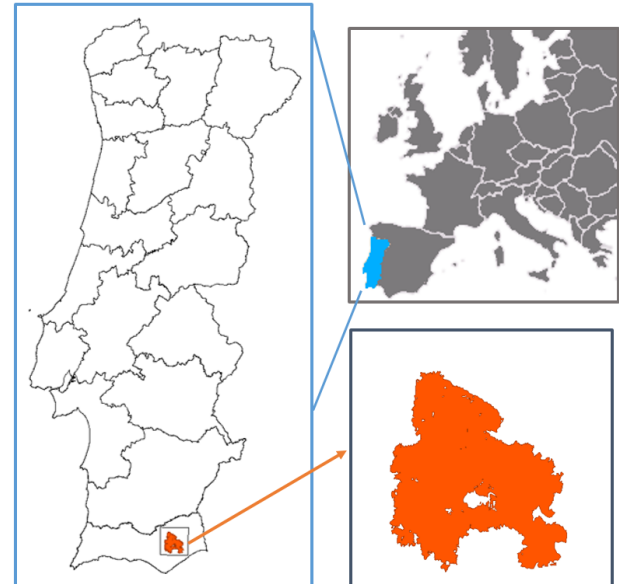
Figure 1. Left panel: map of Portugal with the location of the Tavira wildfire, where orange represents the burned scar and the black frame indicates the study area used in the simulations. Right panels: schematic representation of Europe with Portugal highlighted in blue (top panel) and zoom of the study area (bottom panel).

that year. Since 2012 was a year of extreme drought, the meteorological background conditions were very prone to the occurrence of large fire events (Trigo et al., 2013).

The fire propagated in two distinct phases. In the first stage, from 13:00 UTC on July 18 to 17:00 UTC on July 19, the fire burned about 5,000 ha, representing one fifth of the total burned area. In this phase, the wind direction was highly variable and the fire advanced through rugged terrain, with frequent shifts in the direction of maximum spread until it reached the Leiteijo stream.

In the second stage from 17:00 UTC to 24:00 UTC on July 19 the fire turned into a major conflagration, greatly increasing its propagation speed and burning about 20,000 ha in 7 hours. When the fire reached the Odeleite stream it became orographically channeled, as an increase in wind speed led to fast and intense fire growth towards south, where heavy fuel loads were present. The fire split into two advanced sections heading west and east to the São Brás de Alportel and the Tavira municipalities, with a 10 km wide fire front. In addition, spotting created new fires up to two kilometers ahead of the fire front. All these factors allowed rapid propagation of the fire front while turning suppression extremely difficult.

2.2   Input data

A study area of 30 km x 30 km was defined centered on the burned area (Figure 1) and fine-scaled raster data from various sources were collected and pre-processed in a common
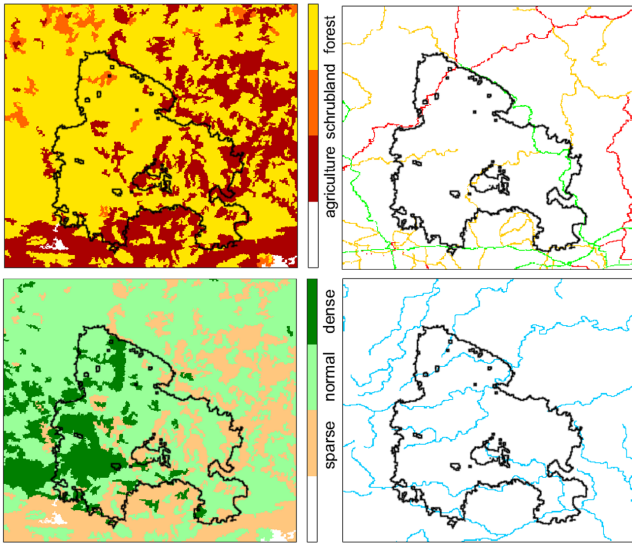
Figure 2. Left column: vegetation type (top) and density classes (bottom) inside the study area as indicated by the discrete colorbars. White corresponds to areas without vegetation. Right column: the roads (top) and waterlines (bottom) identified inside the simulation area. Primary, secondary and tertiary roads are represented, respectively, in red, orange and green. Waterlines are all colored in blue.

Table 1. Assigned values to loadings of vegetation type (p_{veg}) and density (p_{dens}).

categories	p_{veg}
no vegetation	-1
agriculture	-0.4
forests	0.4
shrubland	0.4

categories	p_{dens}
no vegetation	-1
sparse	-0.3
normal	0
dense	0.3

Figure 3. Centroids of the active fires detected by MODIS (top panel) and derived times of burning for the cells inside the burned scar (bottom panel). Colors of the centroids and of the cells represent the elapsed time (in hours) since the beginning of the fire event as indicated in the colorbars. The star represents the fire ignition point reported and the black line the perimeter of the burned area.

format suitable as input for the wildfire simulations. Data include the ignition points, the start and end times of the fire event, the fire perimeters, the burned areas, the surface wind speed and direction, the topography, and information about the landcover (vegetation type, vegetation density, areas burnt in previous wildfires, waterlines and roads).

Patch-slope information was derived from elevation data as obtained from the Digital Elevation Model provided by the Shuttle Radar Topography Mission (Farr et al., 2007).

Hourly wind data were obtained from a regional weather simulation performed with the Weather Research and Forecast model (WRF), version 3.1.1 (Skamarock et al., 2008). The quality of the simulation was previously assessed for wind (Cardoso et al., 2012; Soares et al., 2014). WindNinja (version 2.1.3) (Forthofer, 2007) was then used to spatially model the hourly wind input data taking into account the interaction with topography. The temporal behavior of the wind field was then validated against the information contained in the report by the Portuguese Authority for Nature and Forests (ICNF) (ICNF, 2012).

Fuel type and density were derived by combining information from CORINE Land Cover raster maps at 100 m resolution (CLC2006), the National Forest Inventories produced by ICNF, and the MODIS-based annual Maximum Green Vegetation Fraction (Broxton et al., 2014). Vegetation types were aggregated into four main categories: areas without vegetation, agriculture, shrubland and forests (Figure 2, top left panel). The density of vegetation was also stratified into four

categories: areas without vegetation, areas with sparse, normal and dense vegetation (Figure 2, bottom left panel). As described in section 2.3, for the different categories of vegetation type and density, values of the associated loadings, respectively p_{veg} and p_{den}, were empirically assigned or taken from literature (Alexandridis et al., 2008). Assigned values are listed in Table 1.

Roads and waterlines inside the simulation area (Figure 2, top right panels) were also included in the model by assigning low values to both loadings of p_{veg} and p_{dens}, with $p_{veg} = p_{dens}$. Primary, secondary and tertiary roads were assigned the values $-0.8, -0.7$ and -0.4, respectively, whereas the value of -0.4 was assigned to the waterlines.

Active fire data as identified from satellite were used for the quality assessment of the CA model simulations by evaluating temporal and spatial discrepancies between active fire observations and simulated fire growth. For this purpose, we used the MODIS (MODerate Resolution Imaging Spectroradiometer) active fire product that provides hotspots detected at 1km × 1km pixel resolution, at the time of the satellite overpass. The MODIS sensor on the Terra and Aqua satellites supply daytime and nighttime observations at four nominal acquisition times, thus providing information about the geographical location, date, and time of the detected active fires (Giglio et al., 2003).

For each satellite overpass totally or partially covering the total burned area by the Tavira fire, we used the centroids of the active fire footprints (Figure 3, top panel) to define a polygon confined to the burn scar. Times of burning of cells inside the fire scar were then estimated by bilinearly interpolating between the outer limits of the defined polygons (Figure 3, bottom panel).

2.3 Baseline model

Simulations by the reference CA model developed by Alexandridis et al. (2008) make use of a square grid with propagation to the 8 nearest and next-nearest neighbors (Figure 4). Each cell (or site) is characterized by 4 possible discrete states, corresponding to burning, with fuel not-yet burned, fuel-free, and completely burned cells. The model
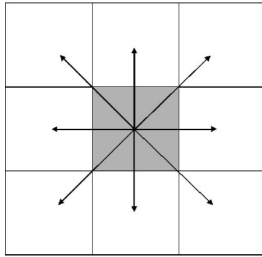
Figure 4. The 8 possible fire spread directions on the square grid.

has 4 possible rules of evolution which take into account fuel properties, wind conditions, and topography. The rules are applied at each time step and are described as follows: Rule 1: a cell that cannot be burned stays the same; Rule 2: a cell that is burning down at present time will be completely burned in the next time step; Rule 3: a burned cell cannot burn again; Rule 4: if a cell is burning down at the present time and there are next-nearest neighbor cells containing vegetation fuel, then the fire can propagate to its neighbors with a probability p_{burn} which is a function of the variables that affect fire spread.

Probability p_{burn} of a given cell depends on a constant reference probability that may be increased or decreased by means of different loadings. The constant reference probability p_0 is the probability that a cell in the neighborhood of a

burning cell (containing a given type of vegetation and density) starts burning at the next time step under no wind and flat terrain. Loadings in turn depend on the vegetation type, p_{veg}, and vegetation density, p_{den}; on topography, p_s; and on wind fields, p_w. In its basic formulation p_{burn} is set as:

$$p_{burn} = p_0(1 + p_{veg})(1 + p_{den})p_w p_s. \tag{1}$$

As described in section 2.2, in order to account for the effect of vegetation, both type and density were stratified into discrete classes, and for each class a constant loading was assigned as specified in Table 1.

The effect of the wind is modeled as:

$$p_w = \exp[V(c_1 + c_2(\cos(\theta) - 1))], \tag{2}$$

where c_1 and c_2 are adjustable coefficients, V is the wind speed, and θ is the angle between the wind direction and the fire propagation direction. As expected, p_w increases when wind and fire directions are aligned.

The probability factor that models the effect of the terrain slope is given by:

$$p_s = \exp(a_s \theta_s), \tag{3}$$

where θ_s is the slope angle of the terrain and a_s is a coefficient that can be adjusted from experimental data. Slope angle θ_s was derived from elevation data, E, according to

$$\theta_s = atan[(E_1 - E_2)/D], \tag{4}$$

where D is equal to the size L of the square cell when the two neighboring cells are adjacent or to $\sqrt{2}L$ when the two cells are diagonal. As expected this topography effect is higher when the fire spreads uphill.

2.4 Modified model

In order to better mirror the role played by the wind in fire propagation, a modification was introduced in the model by means of a new rule that allows propagation to non-adjacent cells with the aim of incorporating the effects due to fire spotting (Figure 5). In contrast with the baseline rule N_1 that at
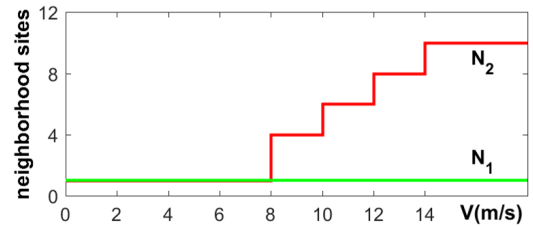
Figure 5. The baseline fire spread rule (N_1) and the new wind propagation rule (N_2).

each time step fire can only spread to its nearest and next-nearest neighbors, according to the new rule N_2, for each
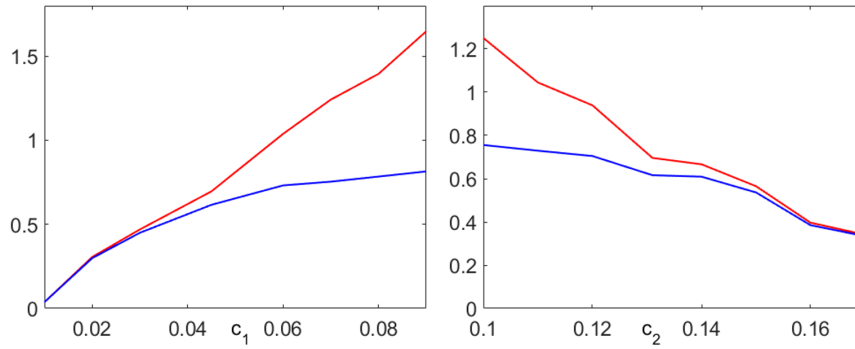
Figure 6. Simulated values of the total burned area (red curves) and of the burned area inside the perimeter of the fire scar (blue curves) in units of the total area inside the perimeter as a function of c_1 for fixed $c_2 = 0.131$ (left panel) and as a function of c_2 for a fixed $c_1 = 0.045$ (right panel).

burning cell at a given time step, fire propagation is modeled according to the two following steps: apply the baseline wind rule and determine the direction(s) of fire spread (if any) for each cell in the next-nearest neighborhood. If: i) according to the previous step, the fire propagates to a new cell, ii) the wind speed at the considered burning cell is above the threshold of 8 m/s and iii) the angle between the wind direction and the displacement vector (from the considered burning cell to the newly ignited cell) is lower than $\pi/10$, then fire also spreads to a number of other contiguous cells (along the displacement vector), the number of ignited cells depending on the wind speed at the considered burning cell (Figure 5).

The model with the new propagation rule N_2 will be hereafter referred to as the modified model.

2.5 Simulations

The landscape was discretized into square cells with size of 100 m and the model free parameters were set according to Alexandridis et al. (2008), i.e. with $p_0 = 0.58$, $a_s = 0.078$, $c_1 = 0.045$ and $c_2 = 0.131$. The time step of the model was set by performing 100 simulations of the propagation of fire inside the observed burned area under no-wind and flat-terrain conditions. The time step was then estimated by dividing the observed time from the starting ignition up to fire containment (46 h) by the mean number of time steps required to burn the entire area. The obtained time step was about 20 minutes.

A sensitivity study was also performed to assess the effects of constants c_1 and c_2 on the propagation of fire (Equation 2). As shown in Figure 6, simulated values of total burned area and of burned area inside the perimeter of the fire scar increase (decrease) with increasing c_1 (increasing c_2). Moreover, above (below) a certain threshold of c_1 (c_2), a progressive departure is observed between the simulated values of total burned area and of burned area inside the perimeter of the fire scar, an indication that the simulated fire is spreading out of the recorded limits. Choice of $c_1 = 0.045$

and $c_2 = 0.131$ (Alexandridis et al., 2008) represents a compromise between burning a large fraction of the area inside the perimeter and spreading a small fraction outside.

The fire event was then modeled using a probabilistic approach based on ensembles of 100 model simulations and the probability that a given cell burns was accordingly estimated by the fraction of runs where that cell was modeled as a burned one. Two different kind of simulations were performed, respectively constrained and unconstrained. In the first kind, burning was confined to the observed burned area by means of an appropriate setting of the model parameters along the boundary of the final observed scar. It may be noted that this setting along the scar boundary is not an artificial device since it reflects the known a posteriori fact that the shape of the scar resulted from effective fire-fighting in locations where changes in fuel types and the presence of roads make fire propagation harder. In the second kind of simulations, no other constraints were imposed besides the lattice domain, i.e., in this case all fire propagation simulations stop by themselves.

3 Results

3.1 Constrained runs

Two different ensembles of 100 simulations were generated, one with the baseline fire spread model and the other with the modified model. Results obtained at four selected stages of the fire are displayed in Figure 7. When using the baseline rule (Figure 7, left panels), and excepting for the slot at 25 h (after ignition) where there is a fair agreement between the simulated burned area and the front lines of the fire as indicated by the hotspots identified by satellite, the simulated burning is well behind the fire front, an indication that the modeled propagation of the fire is too slow. A strong contrast is observed when using the modified model (Figure 7, right panels). In this case, the modeled burned areas spread much closer to the fire front as defined by the hotspots. The
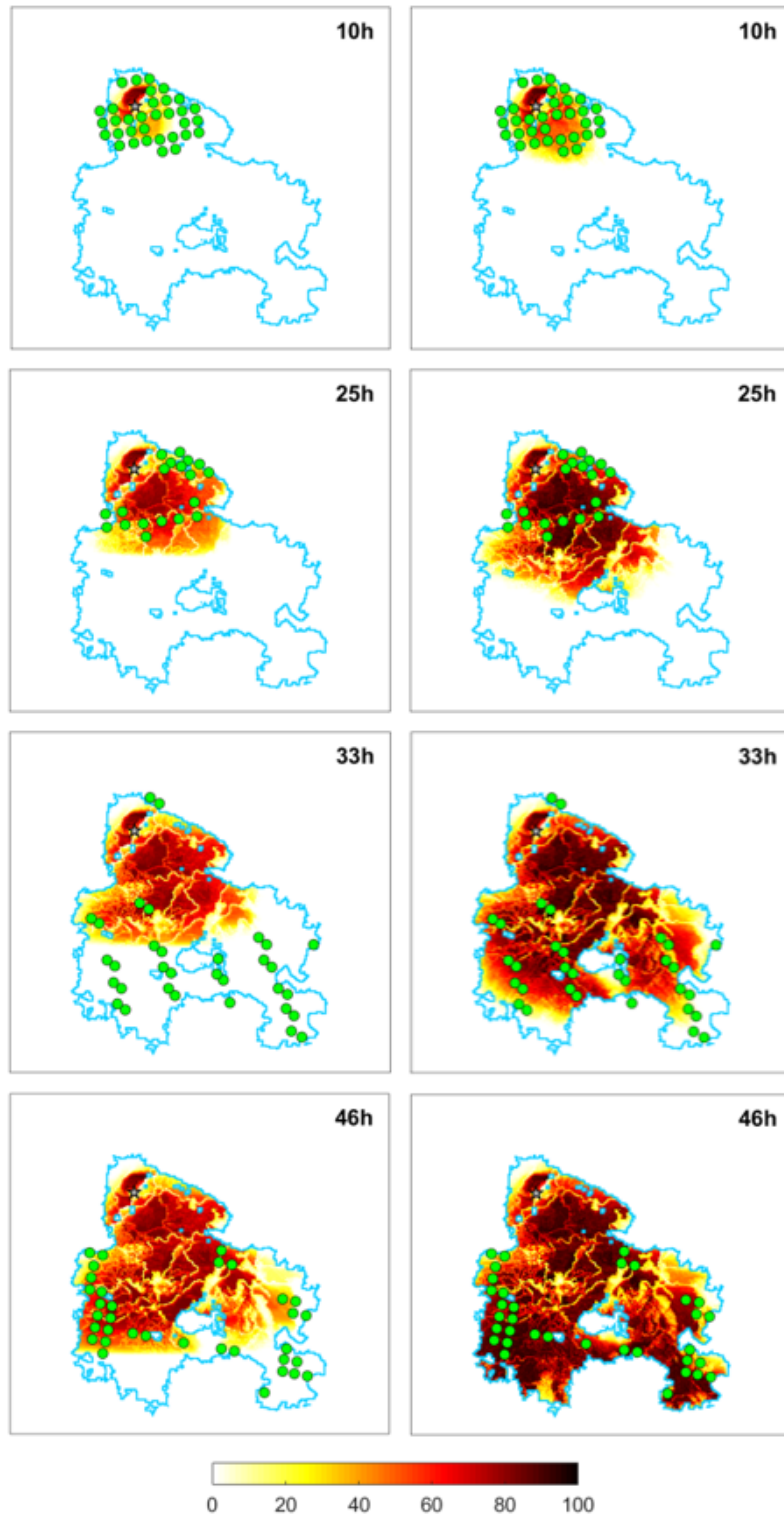
Figure 7. Probabilities of burning (%) for the baseline model (left panels) and for the modified model (right panels). Colors represent the percentage of burned cells as indicated by the color bar in the bottom of the figure and white represents unburned cells. The star locates the fire ignition point, the blue line is the perimeter of the burned area, and the green circles represent active fires as detected by MODIS. Both simulations were restricted to the burned area.
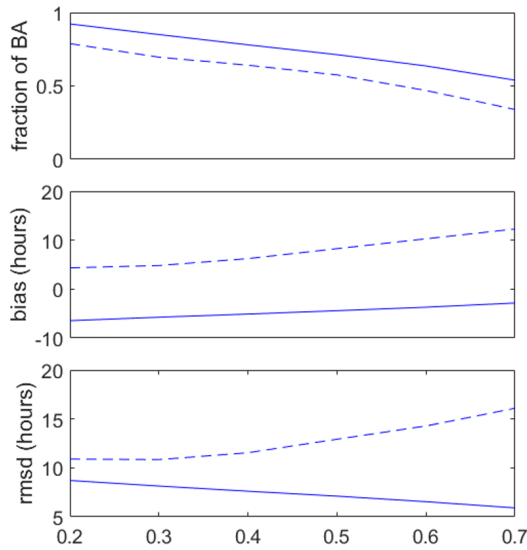
Figure 8. Fraction of the burned area inside the perimeter relative to the total area inside the perimeter of the fire scar (top panel), bias (middle panel) and root mean square difference (bottom panel) as a function of the probability threshold for $c_1 = 0.045$ and $c_2 = 0.131$. The dashed lines correspond to the baseline model and the solid lines to the modified model.

exception is the slot at 25 h (after ignition), where the modeled propagation of fire is faster than the one suggested by the location of the hotspots. On the other hand, it is worth emphasizing that the explosive behavior of fire between slots
5 at 25 h and at 33 h is well simulated when using the new wind propagation rule.

Burned area in each one of the two ensembles was identified by assuming that a given pixel is a burned one when the modeled probability that it burned is larger than a fixed
10 threshold. Each pixel identified as burned was assigned the respective time step as an indicator of the modeled time of burning. Time deviations were then computed by subtracting the times of burning as derived from the hotspots identified by MODIS (Figure 3, bottom panel). Finally, three mea-
15 sures of quality of the simulations were derived for different thresholds of probability, namely the fraction of burned area (relative to the total area inside the perimeter of the fire scar), the bias (simulated time minus time derived from hotspots) and root mean squared differences (between simulated time
20 and time derived from hotspots).

Figure 8 presents results obtained when using the model with the baseline wind rule (dashed lines) and the modified model (solid lines). In both cases, and as to be expected, the fraction of burned area decreases with increasing values of
25 the threshold (Figure 8, top panel), the baseline model always presenting, for each threshold, lower values of burned area than the modified model. The baseline (modified) model presents positive (negative) values of bias for each thresh-

old (Figure 8, middle panel) meaning that, on average, the simulations are late (in advance) when compared with times
30 derived from satellite. In both cases, the bias increases with increasing values of threshold, the baseline model becoming more and more biased and the modified model approaching zero bias, although the rate of increase is smaller than the one of the baseline model. Finally, the root mean square differ-
35 ence (Figure 8, bottom panel) shows an opposite behaviour in the two cases, with values increasing (decreasing) with the threshold in the case of the baseline (modified) model. When considering all together the three measures of quality of the simulations, the modified is better performant than the
40 baseline model and choosing values of threshold between 0.4 and 0.6 represents a good compromise in terms of simulated burned area and simulated time of fire propagation.

Figure 9 presents the spatial distribution of fire propagation and of time deviations (simulated time minus time de-
45 rived from hotspots) for a probability threshold of 0.5. When using the baseline wind rule (Figure 9, upper panels), the model shows a progressive delay in the propagation of fire, the isochrones of fire propagation attaining values larger that 46 h well before the fire front reaches the southern boundary
50 of the scar. This delay reflects in the positive values of the deviations of modeled time of burning from the one derived from satellite observations and it is worth noting that the delay takes place during the explosive stage of the fire between 25 and 33 h (Figure 3, bottom panel). When using the modi-
55 fied model (Figure 9, lower panels) the explosive stage of the fire is much better modeled albeit a too fast propagation of the fire front during the first stage. This behavior is reflected in the deviations that present negative values during the first 12 h and much lower positive values than the baseline model
60 between 25 and 33 h, an indication that the modified model tends to be closer to the observations than the baseline model. The overall behavior of both models is well summarized by the respective values of bias and of root mean square differences: bias of 8.3 h (-4.4 h) of the baseline model (modified
65 model) is consistent with the too slow (too fast) propagation of the modeled fire fronts whereas the root mean square difference of 12.9 h (7.1 h) points to a behavior closer to observations of the modified model.

The improved behavior of the modified model when com-
70 pared with the baseline model is also revealed when analyzing the fraction of burned pixels of the scar in successive periods of 6 h (Figure 10). The most conspicuous feature is the burning of more than 50% of the total amount of burned cells between 30 and 36 h. This explosive stage of the fire is com-
75 pletely missed by the baseline model, whereas the burned area by the modified model reaches 30%. When the fraction of burned area estimated from remote-sensed hotspots is small (between 0 and 6 h, 12 and 18 h, 18 and 24 h) both models tend to overestimate that fraction, especially the
80 modified model. Between 6 and 12 h, the burned fraction simulated by the modified model is close to the burned area estimated from hotspots, whereas the baseline model under-
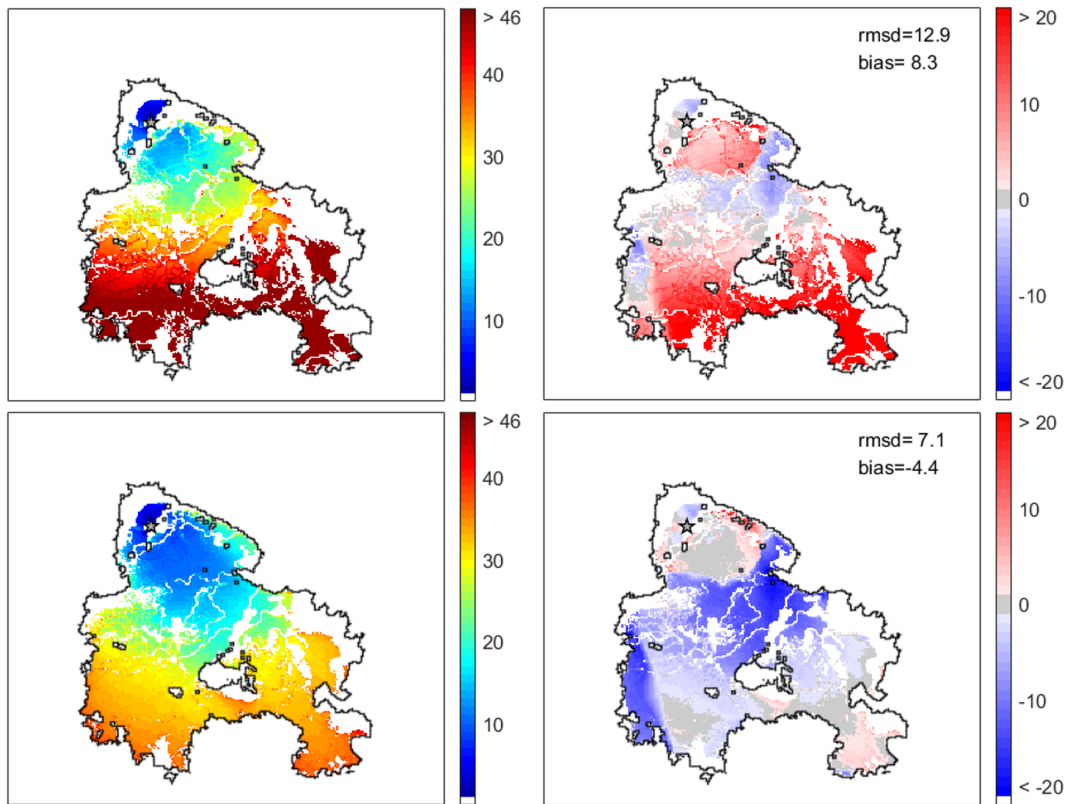
Figure 9. Left panels: fire propagation using a threshold of 0.5 for probability of burning for a set of 100 random simulations of the baseline model confined to the burned area (top panel) and of the modified model (bottom panel). Colors represent the elapsed time in hours after the fire ignites. Right panels: time deviations from the left panels relative to the active fires detected by MODIS. Red (blue) shading corresponds to a progressive delay (advance) in fire propagation observed in the CA model, and light gray to an agreement between the CA model and the MODIS active fires. The star represents the fire ignition point, the black line the perimeter of the burned area and white represents unburned cells.
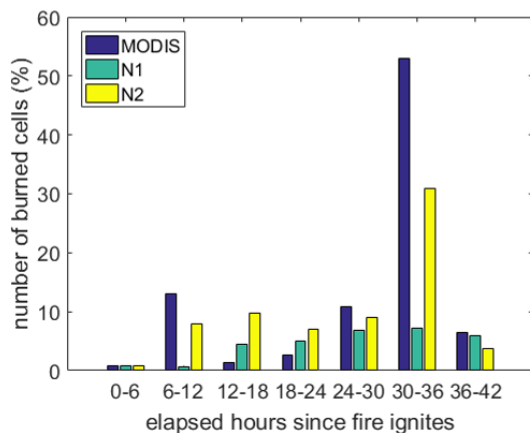
Figure 10. Percentage of the total number of burned cells as derived from active fires (MODIS), the baseline model (N1) and the modified model (N2). Each triplet of columns corresponds to the burned cells identified, respectively, in the intervals [0,6[, [6,12[, [12,18[, [18,24[, [24,30[, [30,36[and [36,42[hours.

estimates that fraction. An opposite behavior occurs in the last interval, between 36 and 42 h, where the fraction simulated by the baseline is close to the fraction estimated from hotspots and the modified model underestimates that fraction.

3.2 Unconstrained runs

When no constraints are imposed, the obtained pattern of burning probabilities (Figure 11, left panel) shows a marked decrease outside the limits of the burned scar and this may be put into evidence by restricting the burned area to cells with a burning probability larger than 80% (Figure 11, right panel). Unconstrained simulations therefore indicate that the probability of burning is lower beyond the actual perimeter of the fire scar as a result of changes in fuel type, topographic effects and the presence of linear interruptions such as roads.
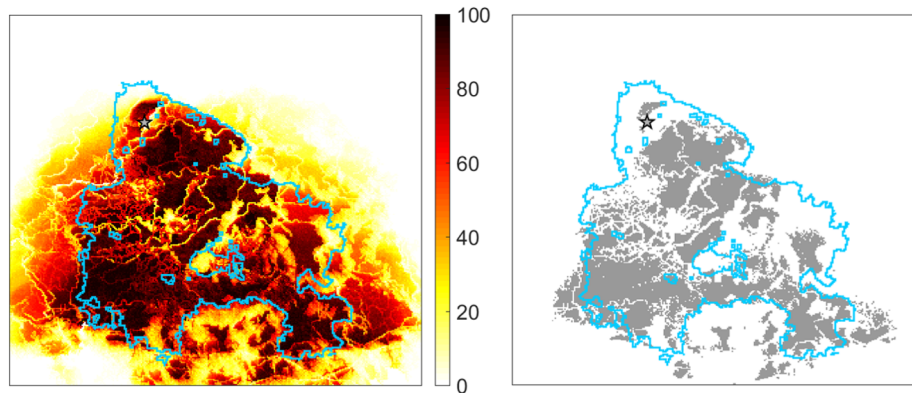
Figure 11. Left panel: probabilities of burning (%) as derived from an ensemble of 100 unconstrained simulations of the modified model. The colorbar indicates the probability of burning. The star represents the fire ignition point, the black line the perimeter of the burned area and white represents unburned cells. Right panel: burned sites identified above a threshold probability of 80%. The blue arrows indicate locations where fire fighting occurred, namely along the lateral sides of the burned scar and populated areas .

4 Discussion

Two different ensembles of constrained runs were generated, based on two models that were analogous except in the wind propagation rule. In the baseline model, the wind rule only applied to the nearest and next-nearest neighbors, whereas in the modified model the neighborhood affected increased with wind speed, reaching up to 10 cells. Results obtained pointed to a progressive delay in the propagation of fire simulated by the baseline model that contrasted with a moderate advance obtained with the simulations by the modified model. The contrast in overall behavior of the two ensembles reflects in the obtained values of bias and root mean square deviations between simulated times of burning of each cell and respective estimated times from hotspots as identified by remote sensing. The value of 8.3 h (−4.4 h) for bias in the case of the baseline (modified) model indicates the overall delay (advance) of the simulation and the improved performance of the modified model is suggested by the value of 7.1 h of the root mean square difference that is more than two hours lower than the value of 12.9 h obtained with the baseline model. Differences between the two ensembles are conspicuous during the explosive stage of the wildfire when about 55% of the area burned between 30 − 36 h after the fire onset. The baseline model simulated less than 10% (out of 55%) of that area whereas the modified model reached 30%. The usefulness of the modified model as a tool to assist fire managers in locating resources for firefighting during a fire event was tested by performing a third ensemble of 100 simulations in which the fire propagation is unconstrained, and the simulations stop by themselves. Results obtained show a marked decrease of probability of burning outside the observed fire scar, suggesting that this type of model may help decison-makers about the placement of the allocated fire-fighting forces during a real fire event (Figure 11, right panel).

The flexibility to the introduction of changes in properties of individual cells (e.g. when imposing constraints to fire propagation along the perimeter of the fire scar) as well as of transition rules (e.g. the proposed one on the effects of wind), together with the required low computational cost (that allows performing a very large number of runs in a short amount of time) make of CA adequate tools to be used, either when planning controlled fires or when making decisions about fighting in an operational scenario. For instance, we are currently developing a mobile application (app) that allows the user to run the proposed modified model over the study area and modify the properties of the individual cells.

5 Summary and Conclusion

In this paper we set up a CA model designed to respond to wind-driven wildfires. The model is applied to a large wildfire event that took place in southern Portugal in July 2012. Besides its relevance in terms of burned area that reached almost 25,000 hectares, the event turned into a major conflagration between 25 and 33 h after the onset, because of orographic channeling accompanied by an increase in wind speed. This explosive stage represented an ideal scenario to test a CA model designed for wind-driven wildfires. The simulation of the wildfire propagation was made using a probabilistic approach based on ensembles of 100 simulations that lets estimating the probability of burning of a given cell by the fraction of runs where that cell was modeled as a burned one.

The proposed CA model with a wind rule that allows fire propagation to non-adjacent cells represents an improvement to the baseline model and reveals potential to be an added value in fire management. Besides introducing the effect of fire spotting, the new wind rule is also an attempt to circumvent the problem of having a fixed time-step for the propa-

gation of fire on a fixed lattice. Results indicate that unconstrained simulations are a useful tool to assist decision makers during a fire event, by providing indications about locations of low burning probability to be selected as appropriate
5 to allocate resources for fire fighting. Currently the model is being tested in different scenarios, namely with the very large fire events that took place in Portugal in June and October 2017.

It is worth mentioning that the transition rules that were
10 used in the CA model do not take into consideration either the state of stress of vegetation or the meteorological conditions. In line with Alexandridis et al. (2011), incorporation of these two aspects is currently being considered by associating probability factors to the Drought Code (DC) and to the
15 Fine Fuel Moisture Code (FFMC), two indices of the Canadian Fire Weather Index System that respectively provide a numerical rating of seasonal drought effects and of the ease of ignition and the flammability of fine fuel at the daily level (Wagner, 1974, 1987; Pinto et al., 2018).
20 Finally, it may be noted that results from the CA models are presented in terms of probability of burning as an outcome of ensembles of runs. This raises the issue of providing information of model uncertainty that is especially relevant if the CA model is to be used as a decision-making support tool.
25 As discussed in Fischhoff and Davis (2014), characterizing model uncertainty involves identifying key outcomes, characterizing variability as well as internal and external validity, and finally summarizing uncertainty. Presentation of the impacts on fraction of burned area, bias and root mean square
30 deviations when choosing different thresholds of probability of burning are a first step towards conveying results of uncertainty. Further steps in this direction will have to involve direct contacts with decision-makers when analyzing other large fire events namely the above-mentioned ones that took
35 place in Portugal in June and October 2017.

Author contributions. JGF performed the study. JGF and CDC wrote, discussed the results and reviewed the manuscript.

Competing interests. The authors declare that they have no competing interests

40 *Acknowledgements.* JGF was supported by the Post-Doctoral grant SFRH/BPD/101760/2014 from FCT, Portugal. Part of this work was also supported by the project BrFLAS - Brazilian Fire-Land-Atmosphere System (FAPESP/1389/2014) funded by national funds through the Portuguese Foundation for Science
45 and Technology (FCT). Part of the data was provided by the FIRE-MODSAT project, financed by FCT, Portugal (Contract EXPL/AGR-FOR/0488/2013).

References

Alexandridis, A., Vakalis, D., Siettos, C. I., and Bafas, G. V.: A Cellular Automata model for forest fire spread prediction: The case of the wildfire that swept through Spetses Island in 1990, Applied Mathematics and Computation, 204, 191–201, https://doi.org/10.1016/j.amc.2008.06.046, 2008.

Alexandridis, A., Russo, L., Vakalis, D., Bafas, G. V., and Siettos, C. I.: Wildland fire spread modelling using cellular automata: evolution in large-scale spatially heterogeneous environments under fire suppresion tactics, International Journal of Wildland Fire, 20, 633–647, https://doi.org/10.1071/WF09119, 2011.

Amraoui, M., Liberato, M. L. R., Calado, T. J., DaCamara, C. C., Coelho, L. P., Trigo, R. M., and Gouveia, C. M.: Fire activity over Mediterranean Europe based on information from Meteosat-8, Forest Ecology and Management, 294, 62–75, https://doi.org/10.1016/j.foreco.2012.08.032, 2013.

Amraoui, M., Pereira, M. G., DaCamara, C. C., and Calado, T. J.: Atmospheric conditions associated with extreme fire activity in the Western Mediterranean region, Science of the Total Environment, 524-525, 32–39, https://doi.org/10.1016/j.scitotenv.2015.04.032, 2015.

ANPC: Tavira/Cachopo/Catraia ocurrence report 2012080021067. National Authority for Civil Protection [In Portuguese], 2012.

Broxton, P. D., Zeng, X., Scheftic, W., and Troch, P. A.: A MODIS-Based 1 km Maximum Green Vegetation Fraction Dataset, J. Appl. Meteorol. Clim., 53, 1996–2004, https://doi.org/10.1175/JAMC-D-13-0356.1, 2014.

Cardoso, R. M., Soares, P. M. M., Miranda, P. M. A., and Belo-Pereira, M.: WRF high resolution simulation of Iberian mean and extreme precipitation climate, International Journal of Climatology, 33(11), 2591–2608, https://doi.org/10.1002/joc.3616, 2012.

Clarke, K. C., Brass, J. A., and Riggan, P. J.: A Cellular Automaton Model of Wildfire Propagation and Extinction, Photogrammetric Engineering & Remote Sensing, 60, 1355–1367, 1994.

CLC2006: The CORINE Land Cover (CLC) dataset produced in 2006, https://land.copernicus.eu/pan-european/corine-land-cover/clc-2006.

Collin, A., Bernardin, D., and Séro-Guillaume, O.: A physical-based cellular automaton model for forest-fire propagation, Combustion Science and Technology, 183, 347–369, https://doi.org/10.1080/00102202.2010.508476, 2011.

DaCamara, C. C., Calado, T. J., Ermida, S. L., Trigo, I. F., Amraoui, M., and Turkman, K. F.: Calibration of the Fire Weather Index over Mediterranean Europe based on fire activity retrieved from MSG satellite imagery, International Journal of Wildland Fire, 23, 945–958, https://doi.org/10.1071/WF13157, 2014.

Farr, T. G., Rosen, P. A., Caro, E., Crippen, R., Duren, R., Hensley, S., Kobrick, M., Paller, M., Rodriguez, E., Roth, L., Seal, D., Shaffer, S., Shimada, J., Umland, J., Werner, M., Oskin, M., Burbank, D., and Alsdorf, D.: The shuttle radar topography mission, Reviews of Geophysics, 45, RG2004, 1–33, https://doi.org/10.1029/2005RG000183, 2007.

Finney, M. A.: FARSITE: fire area simulator - model development and evaluation, Research Paper RMRS-RP-4 Revised, Ogden, UT: US Department of Agriculture, Forest Service, Rocky Mountain Research Station, pp 47, 2004.

Fischhoff, B. and Davis, A. L.: Communicating scientific uncertainty, PNAS, 111 (Supplement 4), 13 664–13 671, https://doi.org/10.1073/pnas.1317504111, 2014.

Forthofer, J. M.: Modeling Wind in Complex Terrain for use in Fire Spread Prediction. Thesis, Colorado State University, Fort Collins, CO, pp 123, 2007.

Ghisu, T., Arca, B., Pellizzaro, G., and Duce, P.: An Improved Cellular Automata for Wildfire Spread, Procedia Computer Science, 51, 2287–2296, https://doi.org/10.1016/j.procs.2015.05.388, 2015.

Giglio, L., Descloitres, J., Justice, C. O., and Kaufman, Y.: An enhanced contextual fire detection algorithm for MODIS, Remote Sensing of Environment, 87, 273–282, https://doi.org/10.1029/2005JG000142, 2003.

ICNF: Recuperação da área ardida do incêndio de Catraia. Tech. report [In Portuguese], http://www2.icnf.pt/portal/florestas/dfci/relat/raa/rel-tec/raai-catraia-2012, 2012.

Panisset, J., DaCamara, C. C., Libonati, R., Peres, L. F., Calado, T. J., and Barros, A.: Effects of regional climate change on rural fires in Portugal, Anais da Academia Brasileira de Ciências (Annals of the Brazilian Academy of Sciences), 89(3), 1487–1501, https://doi.org/10.1590/0001-3765201720160707, 2017.

Pereira, M. G., Trigo, R. M., DaCamara, C. C., Pereira, J. M. C., and Leite, S. M.: Synoptic patterns associated with large summer forest fires in Portugal, Agricultural and Forest Meteorology, 129, 11–25, https://doi.org/10.1016/j.agrformet.2004.12.007, 2005.

Pereira, M. G., Calado, T. J., DaCamara, C. C., and Calheiros, T.: Effects of regional climate change on rural fires in Portugal, Climate Research, 57, 187–200, https://doi.org/10.3354/cr01176, 2013.

Pinto, M. M., DaCamara, C. C., Trigo, I. F., Trigo, R. M., and Turkman, K. F.: Fire danger rating over Mediterranean Europe based on fire radiative power derived from Meteosat, Natural Hazards and Earth System Sciences, 18, 515–529, https://doi.org/10.5194/nhess-18-515-2018, 2018.

Pinto, R. M. S., Benali, A., Sá, A. C. L., Fernandes, P. M., Soares, P. M. M., Cardoso, R. M., Trigo, R. M., and Pereira, J. M. C.: Probabilistic fire spread forecast as a management tool in an operational setting, SpringerPlus, 5, 1205, https://doi.org/10.1186/s40064-016-2842-9, 2016.

Rothermel, R. C.: A mathematical Model for predicting fire spread in wildland fuels. Research Paper INT-115, Ogden, UT, US: Department of Agriculture, Forest Service, Intermountain Forest and Range Experiment Station, pp 47, 1972.

Rothermel, R. C.: How to predict the spread and intensity of forest fire and range fires. General Technical Report INT-143, Ogden, UT, US: Department of Agriculture, Forest Service, Intermountain Forest and Range Experiment Station, pp 161, 1983.

Rui, X., Hui, S., Yu, X., Zhang, G., and Wu, B.: A physical-based cellular automaton model for forest-fire propagation, Natural Hazards, 91, 309–319, https://doi.org/10.1007/s11069-017-3127-5, 2018.

Sá, A. C. L. and Pereira, J. M. C.: Cartografia de Áreas Queimadas em 2009 em Portugal Continental, 2011.

Skamarock, W. C., Klemp, J. B., Dudhia, J., Gill, D. O., Barker, D. M., Duda, M. G., Huang, X.-Y., Wang, W., and Powers, J. G.: A description of the Advanced Research WRF version 3, NCAR Tech. Note NCAR/TN-4751STR, 2008.

Soares, P. M. M., Cardoso, R. M., Semedo, A., Chinita, M. J., and Ranjha, R.: Climatology of Iberia coastal low-level wind jet: WRF high resolution results, Tellus A: Dynamic Meteorology and Oceanography, 66(1), https://doi.org/10.3402/tellusa.v66.22377, 2014.

Sullivan, A. L.: Wildland surface fire spread modelling, 1990–2007. 3: Simulation and mathematical analogue models, International Journal of Wildland Fire, 18, 387–403, https://doi.org/10.1071/WF06144, 2009.

Trigo, R. M., Pereira, J. M. C., Pereira, M. G., Mota, B., Calado, M. T., DaCamara, C. C., and Santo, F. E.: Atmospheric conditions associated with the exceptional fire season of 2003 in Portugal, International Journal of Climatology, 26, 1741–1757, https://doi.org/10.1002/joc.1333, 2005.

Trigo, R. M., Añel, J., Barriopedro, D., García-Herrera, R., Gimeno, L., Nieto, R., Castillo, R., Allen, M. R., and Massey, N.: The record Winter drought of 2011–2012 in the Iberian Peninsula, Bull. Am. Meteorol. Soc., 94(9), S41–S45, 2013.

Trunfio, G. A.: Predicting wildfire spreading through a hexagonal cellular automata model, in: Lecture Notes in Computer Sciences, ACRI 2004, edited by P M A Sloot, B Chopard, A. G. H., vol. 3305, pp. 385–394, Springer-Verlag, Berlin, Heidelberg, https://doi.org/10.1007/978-3-540-30479-1_40, 2004.

Trunfio, G. A., D'Ambrosio, D., Rongo, R., Spataro, W., and Gregório, S. D.: A new algorithm for simulating wildfire spread through cellular automata, ACM Transactions on Modeling and Computer simulation, 22, Article No.6, https://doi.org/10.1145/2043635.2043641, 2011.

Viegas, D. X., Figueiredo, A. R., Ribeiro, L. M., Almeida, M., Viegas, M. T., Oliveira, R., and Raposo, J. R.: Tavira/São Brás de Alportel forest fire report 18-22 July 2012 [In Portuguese], 2012.

Wagner, C. E. V.: Structure of the Canadian Forest Fire Weather Index, Can. Forestry Serv., Publication 1333, Ottawa, Ontario, pp 49, http://www.cfs.nrcan.gc.ca/bookstore_pdfs/24864.pdf, 1974.

Wagner, C. E. V.: Development and structure of the Canadian Forest Fire Weather Index System, Can. Forestry Serv., Technical Report 35, Ottawa, Ontario, pp 48, 1987.